Chapter 6
Abrasive Water Jet Milling

Mukul Shukla

Abstract Abrasive water jet (AWJ) machining and abrasive water jet cutting (AWJC) are widely used, especially where very hard materials like titanium (Ti) alloys, high-strength steel, ceramics, etc. need to be machined or cut. In this chapter, an overview of the abrasive water jet milling (AWJM) process is presented. The essential challenge is at controlling the depth of cut (DoC) produced by varying the important AWJ machining process parameters. Experimental studies, process modeling and control based on FEM, artificial intelligence techniques and regression, and mechanisms of material removal are covered from the recent literature with the focus being on Titanium alloys. Experimental study and nonlinear regression–based process modeling of controlled depth AWJ milling of Grade 2 Ti alloy is also presented. Finally, various challenges including scope of future research in AWJM are highlighted.

6.1 Introduction

In recent times, numerous advanced machining processes have been introduced, giving better quality machining, while being competitively economical and efficient. These processes include those based on lasers, abrasive water jets (AWJ), plasma, and ion beams. AWJ milling which is a form of AWJ machining is gaining wide popularity owing to its speed and flexibility of processing a wide variety of materials. Newer grade of materials possessing superior properties, for example,

M. Shukla (✉)
Department of Mechanical Engineering Technology, University of Johannesburg, South Africa, Johannesburg, South Africa
e-mail: mshukla@uj.ac.za; mukulshukla@mnnit.ac.in

M. Shukla
Department of Mechanical Engineering, MNNIT, Allahabad, UP, India

J. P. Davim (ed.), *Nontraditional Machining Processes*,
DOI: 10.1007/978-1-4471-5179-1_6,

ceramics, composites, super alloys, are being used as alternatives to regular materials, for improved economy and increased quality and functionality. A typical machining application is of Titanium (Ti) and its alloys for aircraft components where the preference is for lighter materials with high strength.

6.1.1 Abrasive Water Jet Machining

Off late, cutting based on abrasive laden water jet and laser beam has proved to be a superior method than other traditional cutting methods. Abrasive water jet cutting (AWJC) is being widely used, especially in cutting of harder or low-machinability materials like Ti alloys, ceramics, metal matrix composites, concrete etc. An AWJ machine typically uses a multi-reciprocating pump as the primary energy source. Treated water is pumped to very high pressures in the range of 4,000–6,000 bar (400–600 MPa). An abrasive (e.g., garnet) is introduced into the water stream from an adjacent hopper and directed to a mixing chamber inside the cutting head. The abrasives are accelerated and exit the nozzle with the water through an orifice of small diameter (ranging from 0.1 to 1.0 mm) [1]. The water coming out of the orifice at high velocity (even beyond 1,000 m/s) is used for applications in cutting/machining of materials including toughened steel, ceramics, Kevlar fiber-reinforced polymers, and Ti among others, by the erosion process [2]. Figure 6.1 depicts the schematic of working of a typical AWJ machine.

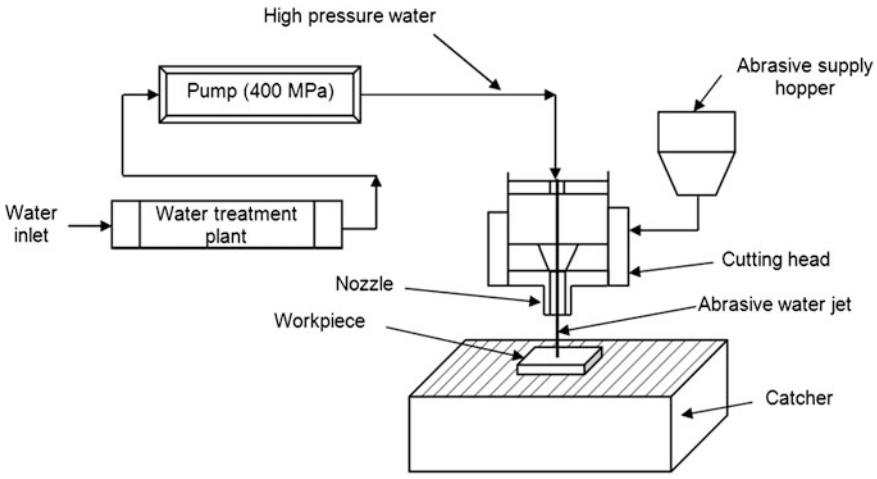

Fig. 6.1 Schematic of a typical AWJ machine

Some of the comparative advantages of AWJ machining over traditional material cutting methods include [3–5]:

1. Marginal thermal stresses or heat generation making it suitable for heat-sensitive materials like plastics.
2. Comparatively faster process.
3. Cut surface is smoother (Fig. 6.2) and requires limited post-processing.
4. Very thin pieces can be cut with least bending or melting.
5. Any contour can be cut (Fig. 6.2) on almost any material.

However, some of the disadvantages of the process are as follows: limited surface finish due to higher abrasive size, noisy, expensive equipment, unsafe if done manually, kerf taper and striated cut surface due to jet characteristics, used abrasives are an environmental hazard and moisture entrapment in workpiece.

Since abrasive water jet milling (AWJM)/C is a comparatively new process, many improvements and developments are ongoing to make the process more economical and standardized. One such application is targeted at AWJ controlled depth milling (CDM) of newer materials like Ti [7]. In-depth practical studies and process modeling for a wide variety of materials would greatly facilitate this implication.

6.1.1.1 Operations

The AWJ machining operations consist of cutting, multi-axis machining, milling, turning, drilling, polishing, etc. as listed below [8].

AWJ Cutting

Cutting is the most popularly used AWJ operation for various industrial applications. AWJ can be used for cutting of advanced materials, where it is required that the heat generated at tool tip should not pass into the workpiece, for maintaining

Fig. 6.2 A typical AWJM sample showing smooth cut contoured surfaces [6, 34]

structural integrity and other physical properties. However, the presence of surface striations and roughness present toward the bottom of the cut surface limit the applications of this technology.

AWJ Multi-Axis Machining

Multi-axis or 3D machining operations on flat objects using AWJs have been challenging owing to the incapability to monitor and control the depth of jet penetration. Two general approaches are generally used in practice for this: (1) using masks or templates to machine complex patterns like isogrid structures using selective pocketing [9] and (2) controlling the jet–workpiece interaction time through control of traverse rate, number of passes, and other process parameters [10]. Figure 6.3a and b, respectively, shows the multi-axis machining operation and multi-axis-machined carbon composite sample.

AWJ Milling

The AWJM occurs when traversing the jets with overlapping multiple passes across the workpiece surface. This multi-pass linear traverse cutting strategy utilizes the principle of superposition of several kerfs to obtain a defined geometry cavity. Several process parameters significantly contribute to the efficiency of the AWJM process as well as the final form of the generated cavities. AWJM of isogrid shapes is conducted to demonstrate the degree of control of milling depth (up to 0.001″) attained using steel masks. Figure 6.4 shows the AWJ-milled slots in a Ti alloy workpiece.

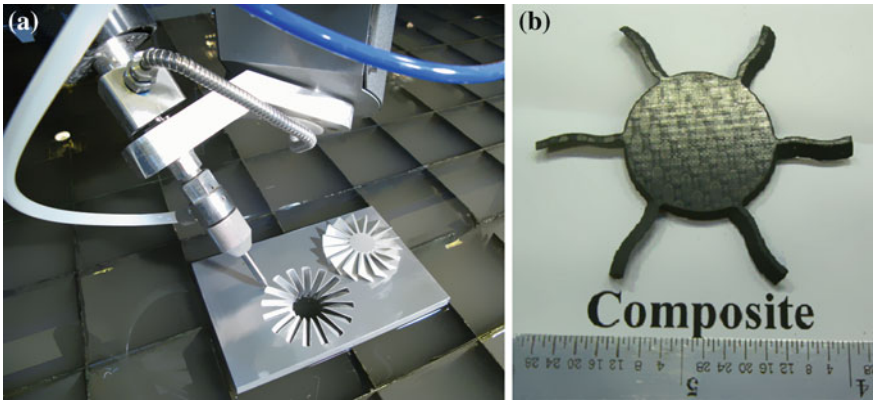

Fig. 6.3 **a** Multi-axis machining operation [wardjet.com] and **b** machined composite sample [11]

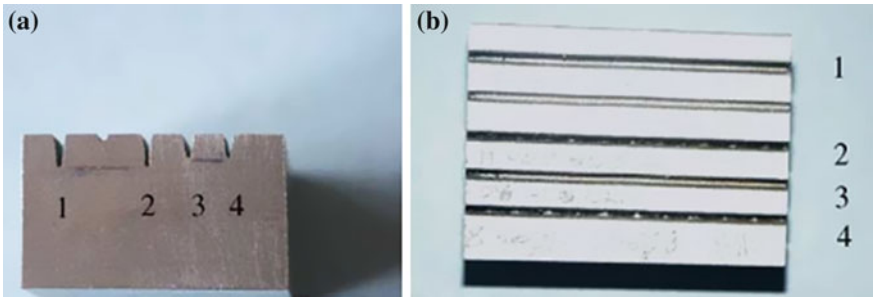

Fig. 6.4 **a** End view and **b** plan view of AWJ-milled slots in Ti alloy [12]

AWJ Turning

AWJ turning has been shown to be a suitable alternative process for turning or an additional preliminary rough turning technology to turn difficult-to-cut hypereutectic aluminum silicon or Ti aluminide alloys (for applications in the aerospace industry). Higher tool life combined with higher material removal rate (MRR), low process temperatures, and less modified material close to the cutting surface gives this cutting technology an edge over the conventional rough turning [13].

AWJ turning like conventional turning consists of spinning a specimen around the axis of rotation and simultaneously traversing the AWJ over the specimen in the desired contour to achieve an axisymmetric shape. The material removal takes place at the face of the workpiece rather than at the circumference at low traverse rates and vice versa. Figure 6.5a and b, respectively, shows the rough AWJ-turned Al specimen at 90° impact angle and with improved surface finish at small impact angle. Figure 6.6 shows the grooved and scalloped grinding wheel generated by the AWJ turning process.

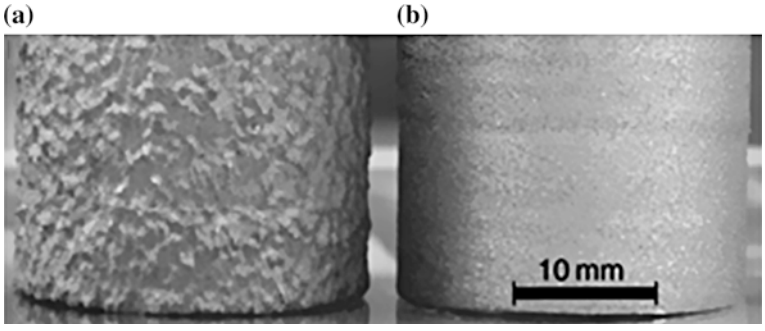

Fig. 6.5 AWJ-turned aluminum specimen at **a** normal and **b** small angle of impact [14]

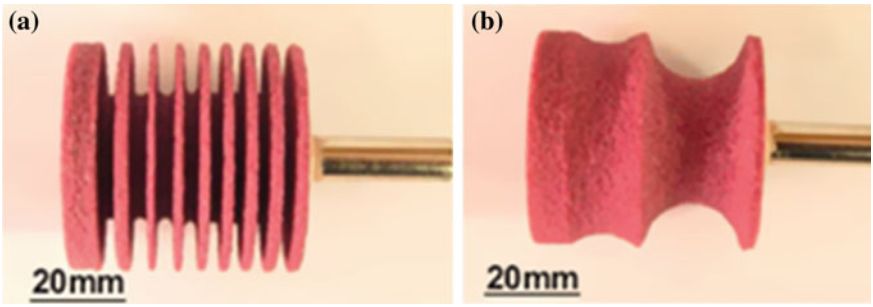

Fig. 6.6 AWJ-turned sample of **a** grooved and **b** scalloped grinding wheel [15]

AWJ Drilling

Hole generation by AWJ is realized by piercing, drilling, or trepanning operations. In piercing, neither the jet nor the specimen performs rotational movement. The jet just penetrates the material axially until it exits past the workpiece. The piercing process comprises of three phases: water jet impact, AWJ penetration, and AWJ dwelling. Size and tolerance of the pierced hole can be controlled by selecting suitable values of process parameters and controlling the dwell time. The longer the dwell, the larger the final hole size.

AWJ drilling is performed with a rotary water jet. The drilling rate linearly increases with an increase in pump pressure and abrasive mass flow rate. Holes can be drilled in different materials up to thickness of 15 cm, but the obtained surface roughness is comparatively low of the order of 2.2 μm.

Hole trepanning is a non-straight cutting process. However, due to the curvature of the cut, the geometry of the jet–material interface is more complex than that of a straight cut. During trepanning, due to the jet trail back, the diameter of the hole increases with increasing workpiece thickness, producing a poor quality hole [16]. The pattern of motion from the piercing location to the wall of the hole and accuracy of the traverse mechanism primarily control the roundness at the top side of the hole.

AWJ Polishing

In AWJ polishing, the sample rotates under the stationary jet and a ring of material is exposed to the jet effect. Here, the abrasives are injected externally in a high-speed hydrojet at shallow angles of attack in between the water jet and the workpiece under high pump pressures. AWJ can polish materials such as ceramics, stainless steel, and alloys. The polished surface quality strongly depends on the size and impact angle of the abrasive grains [8, 29]. A similar process is also used for the removal of coatings and scale.

6.1.1.2 Benefits

AWJ technology offers the following advantages in comparison with the conventional and other non-conventional techniques [7]:

High machining versatility: An abrasive water jet can cut through almost all ductile and brittle materials including many difficult-to-machine materials such as Ti alloys, high-strength advanced ceramics, high-strength steel, metal matrix, and Kevlar composites.

Negligible thermal distortion: The heat generated in AWJ process is instantaneously dissipated by the water. Thereby, there is hardly any temperature rise in the workpiece, leading to minimal changes in the material properties, microstructure, and structural integrity. This characteristic is especially useful for machining thermally sensitive materials such as metals, super alloys, and advanced ceramics.

Small cutting force and speedy setup: The cutting forces being very small, the chances of surface/subsurface damage to the cut material are minimal. Flat-surfaced samples can be directly positioned by laying them on a table without the need of any intricate clamping or tool changes.

Ability to generate contours: AWJs are exceptionally good at 2D machining. However, it is also possible to cut complicated 3D shapes or bevels of any angles and perform 3D profiling.

Eco-friendly: AWJC does not produce any harmful dust or particles that may pose a health hazard if inhaled and is considered to be one of the most environment-friendly machining process.

Availability of raw material: Water is used as the basic working fluid, and the abrasive materials most commonly used are garnet or silica, which are easily available at low cost.

However, AWJ machining also suffers from the following disadvantages:

- Overall the system is expensive in comparison with conventional techniques.
- Moisture entrapment issues;
- Noisy and unsafe;
- Recycling of abrasives.

6.1.1.3 Applications

Because of its technical performance and economics, AWJ machining is used in nearly all modern industries, such as automotive, aerospace, construction, mining, chemical process engineering (Table 6.1), and has numerous other potential applications too. It has been used particularly in pattern cutting of difficult-to-cut materials such as ceramics, laminated glass, and Ti sheets.

Table 6.1 Industrial applications of high-pressure water jets [7]

Industry	Applications
Civil engineering/construction	Cutting reinforced concrete, surface and joint cleaning, vibration-free demolition, soil stabilization and decontamination, water jet supported pile driving
Coal mining	Cutting metal structure, assist in drilling
Chemical and processing	Pipeline cleaning and coating, tube bundle cleaning, vessel, container, and autoclave cleaning
Maintenance and corrosion prevention	Coating removal, emission-free surface cleaning, selective paint sintering
Municipal engineering	Sewer cleaning
Automotive engineering	Deburring of parts
Environmental engineering	Material recycling, emission-free decontamination

6.1.2 Scope of the Chapter

This chapter is primarily limited to AWJ milling–based experimental studies, mechanisms of material removal, and process modeling and control (based on FEM, artificial intelligence techniques, and regression). The chapter mainly focuses on recent literature and AWJ machining of Ti alloys. Experimental study and nonlinear regression–based process modeling of controlled depth AWJ milling of Grade 2 Titanium alloy are presented. Finally, various challenges including scope of future research in controlled depth AWJM are also highlighted. The chapter does not cover the studies on abrasive jet machining, abrasive flow machining, and pure water jet machining.

6.2 Literature Review

AWJM takes place when an AWJ is used to remove material by erosion to a certain limited depth (i.e., not a through cut). AWJM is most feasible for materials that can be eroded more easily than cut (e.g., hard and/or brittle materials and certain tough fiber-reinforced (e.g., Kevlar/Aramid) polymers. AWJM involves the coordination between the bulk MRR and the proper overlap between successive kerf passes. Since the depth of cut (DoC) depends on numerous process parameters, controlling/restraining it while still maintaining desired surface finish has remained a challenge in AWJM applications.

Jet milling was first researched in 1987 by Hashish [17] where he investigated the volume removal rate and parameters that govern the surface topography. The shape of the cut/groove was mainly influenced by the stand-off distance and traverse rate, with higher traverse rates giving better surface topography. Hashish conducted another investigation to compare AWJ milling with traditional milling [18] and studied the effect of various parameters to obtain the best parameter combination that gives high MRR and acceptable surface finish.

A review of the current state of research and development in AWJC was presented in [8, 11, 19]. Another review of research articles of last 5 years on the application of evolutionary techniques in optimizing machining parameters was presented by [20].

6.2.1 Process Modeling and Mechanism of Material Removal

6.2.1.1 Straight Milling

Erosion modeling of AWJM of polycrystalline ceramics providing a relationship for the material effects of dense alumina ceramics on the process of erosion was presented in [21]. There exists a strong correlation between the erosion rate and the ratio of grain size/fracture energy. Experimental investigation of rectangular AWJ pocket milling of alumina ceramics was conducted by [22]. It was found that the depth per cycle decreases with an increase in traverse speed (TS) and reduction in abrasive flow rate (AFR). Experimental determination and feasibility study of using AWJs for CDM of aluminum and Ti isogrid parts used in aerospace and aircraft structures were published in [23]. TS was found to be the most critical parameter affecting the uniformity of milled surfaces and the operative mechanism of material removal. References [12, 24] applied AWJ for CDM of Ti6Al4V alloy. It was concluded that the surface waviness increases with number of passes of the jet over the workpiece.

In a study in AWJ-CDM of Ti alloy, it was found that MRR is high at high impingement angles (around 60°), while surface finish increased with an increase in impingement angle up to 45° [25]. It was demonstrated in [26] that in WJ pocket milling of Ti aluminide, the depth/pass increases with an increase in water jet pressure (WJP) and AFR. Another research study on AWJ-CDM of Ti6Al4V alloy considered particle hardness and shape and found that MRR for all the abrasives (brown aluminum oxide, white garnet grit, white aluminum oxide, and glass beads) is the highest at the lowest TS and decreases rapidly with increasing TS. Glass beads exhibit the lowest rates of the removal [27]. The effect of jet impingement angle and feed rate on the kerf geometry and dimensional characteristics in AWJM of 10-mm-thick SiC ceramic plate was investigated in [28]. They found that the kerf geometry is dependent on the variation in SOD, abrasive particle velocity distributions, and their local impact angles. The ductile erosion mechanism of hard–brittle materials by AWJ was investigated in [29]. Ductile erosion leads to micro-material removal and yields a smooth eroded surface without any fracture.

In another article, the identification and analysis of TS of cutting head in relation to Ti surface topography created by AWJC were performed [30]. Based on surface roughness, the abrasive water jet interaction, mechanism of stock removal,

and a new classification of different qualitative zones were developed, including an often neglected initial zone. An optimal cutting head TS expression was also semi-empirically determined. New relations derived from quadratic sum of the tensile and pressure component of SIG_{def} used to predict a topographic function across the width of the cut were developed.

Based on the jet flow characteristics and erosion theories, Dadkhahipour et al. 2012 investigated the formation mechanisms of channels milled by AWJ on amorphous glass. It was found that the channels were formed through four different zones, i.e., an opening zone, a steady-cutting zone, an unsteady-cutting zone, and a finishing zone. These zones are respectively associated with a secondary viscous flow generated upon the jet impact on the top surface of material, a turbulent flow developed during the penetration of the jet into the material, a transition or laminar flow at the downstream of the jet, and a vortex and damping flow caused by the accumulation of the low-energy solid particles at the bottom of the channel. Bulges are found at the channel bottom and close to the channel wall machined at high nozzle speed as a result of a force induced by the acceleration/deceleration of the moving nozzle when changing direction during the operation. Sawtooth waves are generated on the machined surface for smaller cross feeds [31]. *A study of the micro-channeling process on amorphous glasses using an abrasive slurry jet is presented by* [32]. *The models account for different slurry and workpiece properties*.

The lack of methods for online monitoring of jet penetration (i.e., area of abraded footprint) makes it difficult to control the quality of the AWJM process. Rabani et al. [33] presented a method to control the jet penetration on AWJM, introducing a new concept based on transfer rate of energy (TRE). It links the input jet energy, area of abraded footprint, and jet feed velocity, exploiting its property to remain constant for a particular set of AFR and pump pressure. The input jet energy producing the part erosion is monitored using an acoustic emission (AE) sensor mounted on the workpiece surface, while the jet feed velocity is acquired online from the machine axis encoders. With the preevaluation of TRE as specific response to the set of AWJM parameters, the area of abraded jet footprint can be calculated online. Further, to make the method more powerful, the input jet energy has been related to the process operating parameters, while their constant values have been monitored via a pressure gauge and second AE sensor mounted on the focusing tube. The uniqueness of the proposed monitoring approach is based on the fact that TRE permits to know the amount of adjustments of the jet feed velocity required to keep the jet penetration constant in case any process disturbances occur. This monitoring methodology opens avenues for closed-loop control strategies of AWJM so that complex features can be generated with minimum human intervention.

In AWJM, a flat surface is obtained when the jet cuts single overlapping slots. The resulting surface depends not only on the process parameters but also on the lateral feed between adjacent slots. Many researchers demonstrated the capability of AWJ technology for precision milling operations in different materials using a mask to avoid problems related to the dynamic behavior of the machine. But the

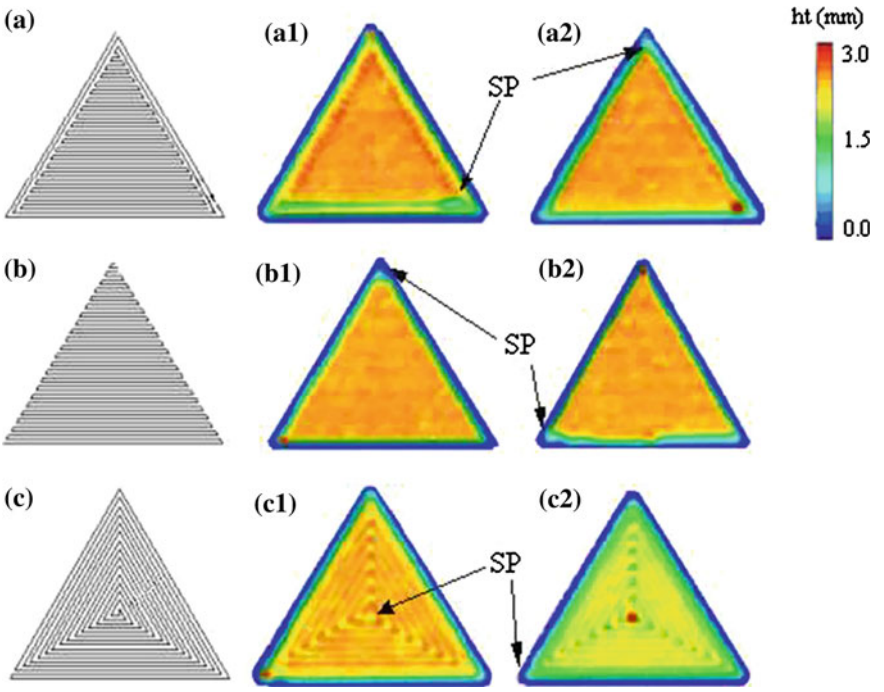

Fig. 6.7 Actual AWJ-milled surfaces for each starting point (SP). **a** Tool path #3, **b** tool path #4, and **c** tool path #5 [34]

limitation related to the use of mask is the additional cost and 2D. Alberdi et al. obtained an experimental model relating the total cavity depth with the depth and width of a single slot and with the lateral feed. Alternative tool paths were also studied aiming to find new strategies to allow maskless AWJ milling (Fig. 6.7) [34].

Another research focused on modeling of slot kerf profile produced by AWJM process consisting of overlapping single slots [35]. A hybrid evolutionary approach combining grammar-guided genetic programming (GGGP) together with genetic algorithms (GA) is proposed as automatic kerf profile model generator based on the maximum depth (h_{max}) and the full width at half-maximum (FWHM) (Fig. 6.8). Both h_{max} and FWHM were modeled using analysis of variance (ANOVA) and regression approach in terms of four important process parameters. The obtained expression after evolutionary system execution is a combination of two exponential functions (Eq. 6.1):

$$h(h_{max}, \text{FWHM}, r) = h_{max}\left(1.21e^{-\left(\frac{1.85r}{\text{FWHM}}\right)^2} - 0.208e^{-\left(\frac{4.45r}{\text{FWHM}}\right)^2}\right) - 12.2\ [\mu\text{m}] \quad (6.1)$$

CDM with AWJs is very difficult to conduct, due to the milled footprint's dependency on both the jet kinematics (e.g., TS or exposure time upon the workpiece and orientation of the jet relative to the target surface) and the jet

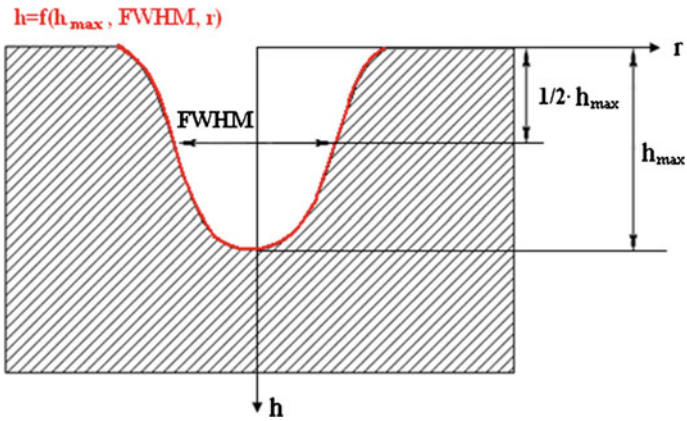

Fig. 6.8 Kerf shape characterization [35]

energy parameters (e.g., WJP, AFR). Anwar et al. [36] conducted modeling, simulation, and validation of AWJ footprint obtained in CDM at various jet TS and pump pressures at 90° angle of attack using the finite element method (FEM). The abrasive particles were modeled with various non-spherical shapes and sharp cutting edges, while the Ti6Al4V alloy extensively used in the aerospace industry is the workpiece material. The interaction between the AWJ plume and the target surface is accounted in the FEM material model by incorporating the effects of strain-rate sensitivity, adiabatic heating, and friction during the particles–workpiece interaction.

6.2.1.2 Multi-axis AWJ Milling

Multi-axis AWJ machining of cylindrical objects is relatively easy to perform by incorporating cutting, turning, and drilling in the same setup. However, 3D machining of flat objects using AWJ has always been a challenge. The capability to monitor and control the depth of penetration in AWJ cutting and drilling determines the effectiveness of multi-axis operations. Both analytical and empirical models have been developed for predicting the depth of penetration in 3D AWJ machining.

A robust model combining the particle kinematics and the constitutive equation for the particle erosion rate was developed. Based on it, a quantitative simulation of the 3D AWJ machining process was performed for local and global machining parameters such as the average DoC, surface roughness, and waviness. The validity of the 3D surface features generated through the model for different processes (such as drilling and cutting) was verified experimentally for glass, Ti, and other metals [37, 38]. Experiments were performed to test the application of 3D axis nozzle control for cutting 3D profile parts [39].

WJC and AWJC can be performed even at pressures up to 690 MPa [40] although normally available commercial systems are only capable of working at a maximum pressure of 379 MPa. Superior quality surfaces were produced at increased pressure, and the abrasive consumption was also significantly reduced. Reference [41] described the AWJC beyond the current industrial pressure limits. Firstly, the factors that limit the water pressure were discussed. Secondly, the jet formation was considered by addressing the effects of the geometry of the upstream tube and the orifice. Finally, the AWJC process was described in terms of energy transfer efficiency. There is an optimum abrasive load ratio over which the cutting ability of the jet decreases due to the less efficient power transfer from water jet to the abrasives.

A wide range of geometries that can be formed using multi-axis AWJ for different materials (carbon fiber composites used in aircraft fuselages to metal matrix composites) were studied by [11]. The influence of abrasive morphology and mechanical properties on workpiece grit embedment and cut quality in AWJC of a Ti alloy was investigated by [42]. Using profilometry, scanning electron microscopy (SEM), and energy dispersive X-ray analysis (EDX), grit embedment, surface waviness and roughness, and abrasive–surface interactions were evaluated. It was concluded that no significant variation in cut surface quality or abrasive particle embedment was observed in spite of using vastly different types of abrasives.

Kong et al. proposed a generic mathematical model applicable to different machine systems, with the benefit of simplicity by having fewer variables, for predicting maskless water-jetted footprints for arbitrarily moving jet paths [43]. This innovative footprint modeling approach has the key advantage of being independent of the properties of the workpiece material and/or machine setup, since it calibrates the specific etching rate. By considering any orientation of the jet plume vector relative to the target surface, this approach becomes a powerful tool for the development of advanced jet path strategies to enable AWJM of complex geometries.

A design of experiments (DOE) approach was taken, considering variables such as WJP, stand-off distance, TS, nozzle orifice diameter, AFR, and tool path step over distance in 3D AWJ pocket milling of Inconel 718. DoC and pocket geometry were the responses [44]. The results showed that WJP has a nonlinear behavior and is the most important variable for controlling the DoC and geometrical errors. Also, nozzle diameter and interaction between feed rate and abrasive mass flow are critical factors affecting the DoC.

6.2.2 DoC Modeling

Evans et al. presented an erosion model capable of predicting the DoC by impact damage in ceramics in the elastic–plastic response regime [45]. This model was adopted by [46] to obtain closed-form expression for the maximum DoC. Instead

of using the typically used vertical cutting force monitoring which is costly and impractical, the online DoC monitoring based on the AE response was modeled [47]. It was established that AE is the most suitable technique for AWJ monitoring owing to its signal having high sensitivity to the DoC variation. A model for predicting the DoC in both oscillation and normal cutting mode was developed in [48]. Their experimental results showed that for ductile materials, nozzle oscillation during cutting at smaller angles and higher frequencies leads to efficient erosion process.

Other experimental DoC studies with controlled nozzle oscillation in AWJC of alumina ceramics were reported in [49, 50]. For the chosen cutting parameters, it was established that a high oscillation frequency (10–14 Hz) along with a low oscillation angle (4–6°) maximizes the DoC. Further, nozzle oscillation at small angles improved the DoC by up to 82 % on proper selection of cutting parameters. In [35], a model to predict the kerf profile (in terms of maximum cutting depth and width at the half of maximum modeled as a Gaussian function) in AWJ slot milling in aluminum 7075-T651 was introduced. The definition of an equivalent instantaneous traverse feed rate along the jet trajectory models the effect of jet acceleration. The model is capable of predicting the kerf profile at constant and variable traverse feed rate due to direction changing trajectories.

S. Harris in his article 'Abrasive water-jet model could enable lower-cost milling,' in The Engineer Online (Nov 25, 2011), highlights that new research could enable lower-cost milling on difficult materials using adapted water jet cutting machines [6]. Fluctuations in water pressure and geometry of abrasive particles mean that AWJM creates surfaces with variable depths. Engineers from research company Tecnalia and the University of the Basque Country in Spain have now developed a model for predicting and controlling the DoCs made by an AWJ machine, which was previously difficult to predict. They used information on process parameters as well as machine acceleration, tool path, and materials, to predict the depth at every point of machined surface (Fig. 6.9). This model is also used to find the optimum process parameters and milling strategy to reach a desired depth in any material and redesign AWJC machines to make them suitable for milling. However, in this report, there is no mention of the achievable surface finish, manufacturing of 3D forms, and comparison of machining time compared to conventional machining.

6.2.2.1 Simulation and Modeling

Experimentally, the eroded material volume loss may be measured and the erosion mechanism also investigated by analyzing the worn surface and erosion conditions. However, erosion is a complex phenomenon, governed by various process variables. Thus, it becomes practically very difficult to comprehend all this experimental information. Computer modeling allows 'virtual experiments' to be carried

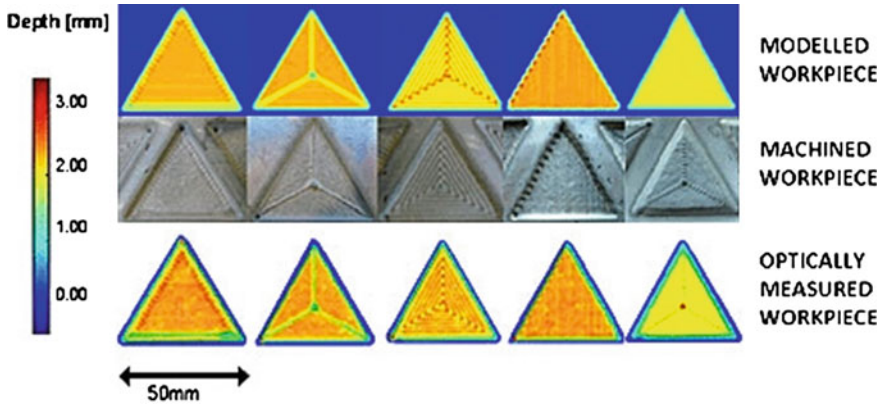

Fig. 6.9 Predicted and controlled DoCs made by an AWJ machine [6, 34]

out under controlled conditions and provides an effective method, complementary to experimental techniques, for a fundamental understanding of the process [51].

A novel approach was presented for modeling of 3D topography generated by AWJC [52]. The 2D topography at different depths of the cut surface was generated by considering the trajectories on the cutting front and the randomly impacting abrasive particles at the cut surface walls. Several 2D profiles generated in each region of cut were superimposed to obtain a net 3D topography. The nature of these 3D profiles was analyzed and validated using power spectral density analysis. In [53], theoretical and experimental studies to model the DoC based on the tilt angle of cutting head were conducted. The model was verified to be widely applicable on a variety of materials and established to be very reliable.

AI Techniques

Fuzzy set theory for selection of levels of the main AWJC parameters for a required DoC was applied in [54]. A neurogenetic approach to adaptively control the AWJC process to model the DoC and derive the optimum parameter settings by accounting for varying diameter of focusing nozzle was presented in [55]. Hybrid artificial neural network (ANN) and simulated annealing (SA) techniques were applied by Zain et al. [56] to estimate optimal process parameters considering a wide range of process parameters. They also integrated the soft computing techniques SA and GA to estimate optimal process parameters that lead to a minimum value of surface finish in AWJC [57]. The estimation of optimal solution using the integrated approach needs a smaller number of iterations compared to individual SA and GA optimization and yields improved machining performance in comparison with experiments and regression modeling. Vundavilli et al. [58] developed a fuzzy logic (FL)-based expert system for prediction of DoC in AWJ machining. It is important to note that the performance of the FL depends on its

knowledge base. The following three FL approaches were used: (1) Mamdani based, (2) the database and rule base of the FL-system are optimized, and (3) the total FL-system is evolved automatically based on binary-coded GA. The accuracy predicted by the automatic FL-system is better than that of other two FL-systems. The expert system eliminates the need of elaborate experimentation, to select the most influential parameters affecting the DoC in AWJ machining.

FEM Based

Various authors have attempted to address the problem of modeling of material removal in erosion using numerical methods based on the finite element method (FEM). Numerical methods although are unable to provide a detailed microscopic insight into the cutting and/or plowing phenomenon of AWJM. Nevertheless, they are highly advantageous as they are capable of simulating the erosion or machining behavior under different conditions (type of material, particle speed, size, shape, impact angle, etc.), thus leading to significant cost reduction, as against the equivalent experimentation [51, 59]

Single Particle

AWJ machining was modeled using FEM and explaining the abrasive particle–workpiece interaction [60]. Single-particle impact modeling in AWJ machining was conducted by [61–63]. In their research, [64] attempted to predict the crater profile produced by single-particle impact for CDM using FEM, rather than first performing the simulation of full jet plume impingement. The main objective of this article was to simulate and experimentally validate the crater profile at different impact angles of abrasive particles in water jet for Ti-based Ti 6Al 4V superalloy.

Multi-Particle

A modified model was presented from Finnie's model for AWJ erosion. This modified model could even deal with curved surfaces and simulated multiple particle erosion [65]. Study of multi-particle solid particle erosion of metallic targets was reported by [66, 67]. Further references on single- and multi-particle erosion modeling using FEM are listed by the author [51]. They conducted FEM-based multi-particle (twenty) impact modeling for erosion in AWJ machining of Grade 5 Ti alloy. The influence of abrasive particle impact angle and size, and velocity on the crater sphericity and depth, and erosion rate has been investigated.

CFD Analysis

Liu conducted computational fluid dynamics (CFD) modeling for ultrahigh velocity AWJs using the commercial flow solver software, Fluent [68]. The

dynamic characteristics of the jet flowing downstream from a fine nozzle were then simulated under both steady state and turbulent, and two- and three-phase flow conditions. The jet characteristics lead to a fundamental understanding of the kerf formation phenomenon in AWJC. Wang (2009) [49] also conducted a similar simulation study of the jet dynamic characteristics using CFD. Wang and Wang (2010) [69] conducted theoretical analysis and developed a two-fluid flow model based on the basic conservation principles. They analyzed quasi-two-dimensional flow field outside the nozzle used in AWJM. A control volume method based on a phase-coupled algorithm was used to solve the coupled pressure–velocity equations.

6.3 Materials and Methods

Ti Grade 2 one of the four unalloyed, commercially available pure Ti variants has the following composition: hydrogen 0.01 %, nitrogen < 0.03 %, carbon < 0.08 %, oxygen < 0.25 %, iron < 0.3 %, Ti balance [70]. It has almost similar properties to Grade 5 alloy (the most widely used Ti alloy) but has relatively low strength and is available at a significantly cheaper price. Some of the unique properties of Grade 2 Ti alloy include:

- Combination of strength, ductility, and toughness;
- Heat treatable, easy to fabricate and weld;
- Can be used at temperatures below 400 °C without loss of physical properties;
- Good tensile properties even at high temperatures.

Ti Grade 2 finds applications in aircraft structures and engine parts, prosthetic devices, turbine blades, marine hardware, desalination equipment, heat exchangers, condenser tubing, etc. [70].

The AWJ-CDM experiments were performed on an ultrahigh pressure, ultrahigh speed, computer numerically controlled, Flow MACH 4 4020b water jet cutting machine (Fig. 6.10). It is equipped with a dynamic XD (to cut straight without the taper effect) 5-axis cutting head (Fig. 6.11) and ultrapierce attachment (for assistance in hole piercing), making it one of the most modern machines available commercially [71]. The specifications of the machine are as shown in Table 6.2.

Various parameters affect the AWJC process. These include—TS of head, jet impact angle and diameter, operating WJP, orifice stand-off distance, AFR and properties (shape, size, hardness, etc.), number of jet passes, etc. [74]. Studying the full variety of AWJ parameters at different levels in a full factorial experimentation would require considerable time and material and is thus infeasible. A DOE-based approach was used in this study to ensure that a larger variety of process parameter combinations are studied with minimum number of experiments [75].

Fig. 6.10 A typical Flow MACH 4 4020b AWJ machine [72]

Fig. 6.11 Typical cutting head of Flow MACH 4 4020b AWJ machine [73]

The three most important parameters were selected based on available literature and machine processing limitations. The three parameters investigated in the present research along with their four levels are given in Table 6.3.

Table 6.2 Typical specifications of Flow MACH 4 4020b

Parameters	Specifications
Operating pressure	0–600 MPa (6,000 bar or 87,000 psi)
Orifice	0.381 mm
Nozzle	1.016 mm
Traverse speed	0–12.7 m/min
Table size	3 × 2 m
Power	50 HP

Table 6.3 Experimental parameter settings

Parameter	Levels
Water jet pressure (P_w)	100, 250, 400, 550 MPa
Traverse speed (U)	2.33, 3.25, 4.08, 5 mm/s
Abrasive mass flow rate (m_a)	0.317, 0.363, 0.408, 0.454 kg/min

During experimentation, the following parameters were kept at a constant value: number of jet passes—1, garnet abrasive size—#80 (180 μm), nozzle stand-off distance—5 mm, and angle of attack—90°. The Ti workpiece was in the form of a flat plate of dimensions 230 × 90 × 38 mm. A 2.5 mm constant distance was maintained between the consecutive slots/cuts of 15–40 mm length (Fig. 6.12). A full factorial experiment was performed with the three parameters set at four levels each making it a total of 64 experiments/trials. The experiments were replicated twice to account for errors if any. The DoC was measured using a digital Mitutoyo Vernier scale (least count = 0.1 mm). Owing to brevity, only partial experimental parameter settings and measured DoC values of the 2nd replicate, along with the regression model predicted and the % error between experimental- and model-predicted values, are included in Table 6.4.

6.4 Data Analysis and Modeling Results

Majority of the DoC models require prior information of the material's properties such as the material's flow stress which cannot be easily determined without experiments. Hence, the energy approach [76, 77] was used in the present work owing to its ease of use and generalization for any material.

$$h = K\frac{m_a^x P_w^y}{d_j \rho_w U^z} \tag{6.2}$$

where K is a constant, h is the DoC, m_a is the abrasive mass flow rate, P_w is the WJP, d_j is the jet diameter, ρ_w is the density of workpiece, and U is the jet TS. The constants of Eq. (6.2) were then derived for modeling using the nonlinear

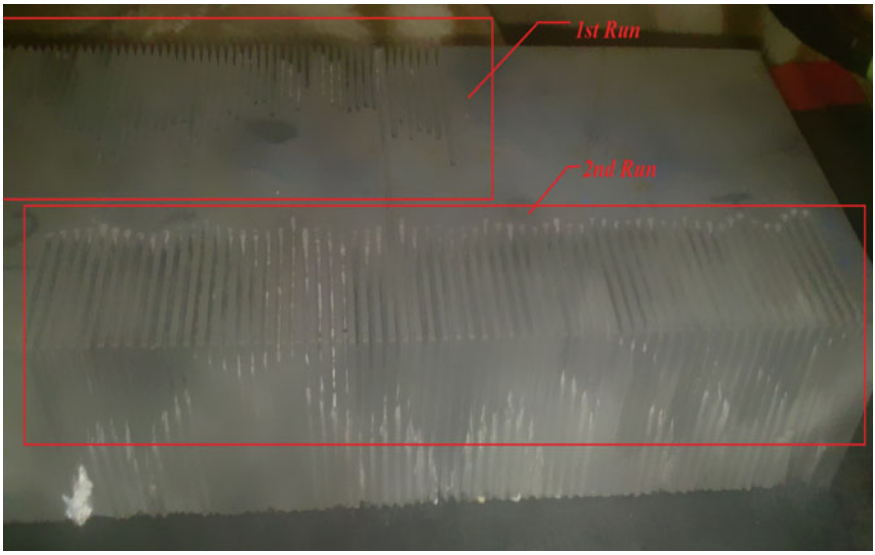

Fig. 6.12 Controlled depth AWJ-milled Ti workpiece [7]

regression software NLREG [78]. Based on the experimental results, the following nonlinear regression equation (Eq. 6.3) was generated (at 95 % confidence level):

$$h = 2.8109 \frac{m_a^{0.668381} P_w^{0.847245}}{d_j \rho_w U^{0.764906}} \tag{6.3}$$

From a comparison of coefficient of determination (R-sqr) values (Table 6.5), it can be observed that the first replicate's results did not give a very good fit with 86.69 % coefficient of determination (at a confidence level of 95 %). The second replicate, however, yielded improved results with a better coefficient of determination at 95.83 %. The mean coefficient of determination of the two runs was found to be 94.94 %. The percentage error is the ratio of the difference between the experimentally measured DoC and the regression model–predicted DoC to the experimental DoC. This is obtained from an average of all the trials in the two experimental runs. The maximum DoC deviation is the maximum difference between the experimentally measured DoC and the model-predicted DoC out of the full 64 cuts.

The average coefficient of determination was found to be 94.94 % which can be interpreted as the likeliness of obtaining similar results in future experiments or applications. This can be interpreted that if the above nonlinear model is used, the results or resulting DoC will have a 94.94 % likeliness of being as predicted. A linear regression model (Eq. 6.4) was also fitted from the experimental data to predict the DoC as follows:

$$h = 5.64 + 22.8\, m_a + 0.0417\, P_w - 3547\, U \tag{6.4}$$

Table 6.4 Select experimental parameter settings, measured and estimated DoC

Run	m_a (kg/min)	P_w (MPa)	U (m/s)	DoC–2nd Run (mm)	Estimated DoC (mm)	% error
1	0.317	100	0.005	2.0	3.72	−86.11
2–4	–	–	–	–	–	–
5	0.317	250	0.00233	15.2	14.49	4.66
6	0.317	250	0.00325	12.4	11.25	9.30
7	0.317	250	0.00408	11.0	9.45	14.13
8	0.317	250	0.005	8.9	8.09	9.10
9	0.317	400	0.00233	23.2	21.58	6.98
10–14	–	–	–	–	–	–
15	0.317	550	0.00408	19.3	18.42	4.55
16	0.317	550	0.005	15.1	15.78	−4.49
17	0.363	100	0.00233	6.8	7.30	−7.35
18–30	–	–	–	–	–	–
31	0.363	550	0.00325	25.0	24.02	3.94
32	0.363	550	0.00233	31.6	30.94	2.08
33	0.408	550	0.00233	Through	33.46	–
34	0.408	550	0.00325	28.4	25.97	8.57
35	0.408	550	0.00408	22.0	21.81	0.88
36	0.408	550	0.005	20.4	18.68	8.44
37	0.408	400	0.005	14.3	14.26	0.27
38	0.408	400	0.00408	17.7	16.65	5.93
39	0.408	400	0.00325	20.0	19.83	0.87
40–52	–	–	–	–	–	–
53	0.454	250	0.005	10.0	10.29	−2.85
54	0.454	250	0.00408	14.0	12.01	14.22
55	0.454	250	0.00325	14.8	14.30	3.38
56	0.454	250	0.00233	19.7	18.42	6.48
57	0.454	400	0.00233	29.0	27.44	5.39
58–62	–	–	–	–	–	–
63	0.454	550	0.00325	28.9	27.89	3.50
64	0.454	550	0.00233	Through	35.93	–

Table 6.5 Statistical analysis of experimental data

Run	R-sqr (%)	% error	Max DoC deviation (mm)
1st run	86.69	35.5	11.7
2nd run	95.83	7.4	4.9
Average	94.94	9.04	4.9

The adequacy of the above regression model was also verified, and the coefficient of determination (R-sqr) was found to be 83 %. As expected in comparison with the nonlinear model, the linear model is unsuccessful to accurately model the DoC in AWJ-CDM.

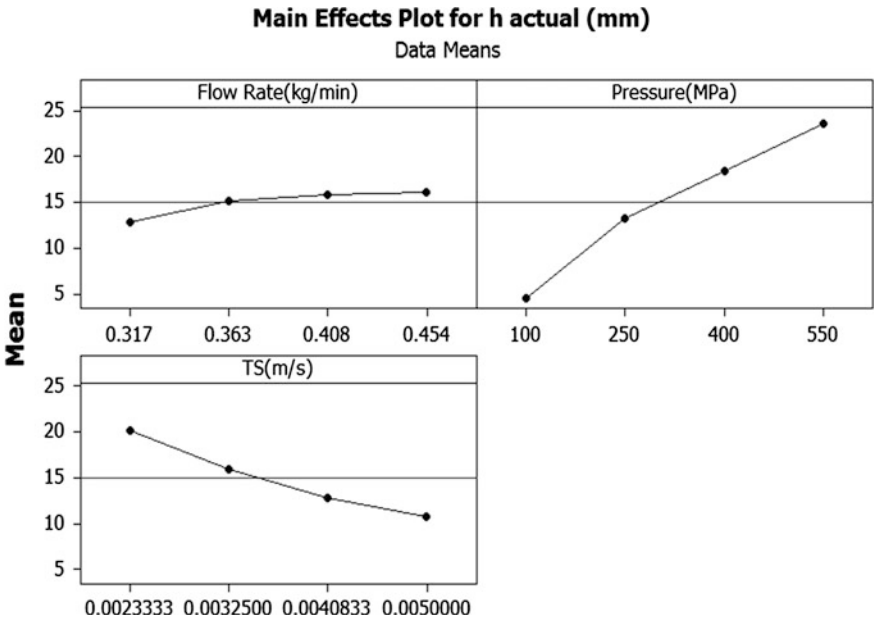

Fig. 6.13 Main effects plot for mean experimental DoC at different settings of the three AWJM process parameters

From Fig. 6.13 of the main effects plot (drawn using the Minitab statistical software [79]), it can be visualized that the WJP had the most dominant effect on DoC, followed by the TS and AFR. As the WJP and AFR increase, the DoC also increases. However, the impact of WJP on DoC is much more significant than AFR. Since the water pressure is the main source of energy in the water jet, an increase in this energy will mean that the jet has an increased eroding power which leads to an increased DoC. The decrease in DoC due to an increase in TS can be explained by the fact that the longer the time is, the more the abrasives are exposed to the surface being cut, and deeper will be the DoC. Increasing the TS/feed rate means decreasing this jet-to-material exposure time and thus a decrease in the depth of the resulting cut. The slightly nonlinear graph of the three process parameters with the DoC suggests that they are related slightly nonlinearly and justifies the adequacy of the nonlinear model (Eq. 6.3) for DoC prediction.

Although the DoC results of the two replicates differed largely in few sporadic cases, the overall average % difference between the results from the two experiments was found to be 0.67 % which can be treated as fairly acceptable. Thus, the experimentation can be considered as being fairly repeatable. Further research investigations on the improvement of this aspect are still ongoing.

6.5 Conclusions and Future Research

The purpose of this chapter was to review the advances in the field of abrasive water jet milling and to develop an abrasive water jet milling DoC prediction model for Grade 2 Ti model. The ultimate idea is toward controlled depth cutting for milling of free-form shapes using AWJs.

Finally, the further challenges and scope of further research in the field of abrasive water jet milling are compiled in this section. This study cannot be complete if surface quality studies are not conducted simultaneously. For these results to be more useful, machining studies constrained with surface quality requirements must be conducted [80, 81]. Optimization and modeling studies to find the optimum operating parameter values for different materials with constrained surface finish requirements are also required [82, 83]. The models can be extended to include additional critical quality attributes such as surface roughness of samples, micro-structure, material embedment, etc. and process parameters such as abrasive type, abrasive grit, tool paths, etc. Influence of attributes such as particles' shape, rotation, multiple overlapping impacts, and effect of slurry jet hydrodynamics can be further investigated in AWJM.

To enhance the cutting performance, various new techniques have been proposed. These include forward angling the jet, controlled nozzle oscillation, and multi-pass cutting and need to be further explored. Studies on DoC using the advanced machines need to include the angle of attack as it has a significant impact for ductile materials. Modern machines can now cut at different angles (3D or multi-axis machines). Exploring the possibility to sculpt any free-form-shaped object is essential as done in conventional milling [84]. Alternative technologies to overcome the grit contamination problem need to be explored. Rabani–AWJ as a versatile effective machining technique requires an accurate controlled monitoring solution to diversify its capabilities throughout industries. However, little attempts have been made for fully automatic monitoring of AWJ milling so far to develop appropriate closed-loop control strategies for AWJ milling.

Many improvements and developments are ongoing to make the AWJ machining process more economical and standardized. In-depth experimental studies combined with process modeling for a wide range of materials would greatly facilitate this mission.

Acknowledgments The financial assistance provided by the Faculty of Engineering and Built Environment, University of Johannesburg, in conducting the experimental studies is greatly acknowledged. Thanks are also due to Dr T U Siddiqui, Dr P B Tambe, Mr Naresh Kumar, and Mr R Gudani, my research students, and to Mr Deon of SA Stainless, Johannesburg, for allowing to conduct experiments on his Flow AWJ machining center.

References

1. WaterJets (2012) www.waterjets.org. Last accessed December 2012
2. Developments in Abrasive WaterJet Technology (2012) http://www.wjta.org/wjta/New_Developments_etc.asp. Last accessed December 2012
3. WaterJet Machining (2012) http://www.nottingham.ac.uk/nimrc/research/advanced manufacturing/waterjet-machining.aspx. Last accessed December 2012
4. Fowler G (2003) Abrasive water-jet-controlled depth milling of titanium alloys. PhD Thesis, Nottingham University, pp 4–56
5. Hashish M (1987) Conference on wear of materials. In: Proceedings of Internet Texas, ASME, NY, pp 769–776
6. http://www.theengineer.co.uk/production-engineering/news/abrasive-water-jet-model-could-enable-lower-cost-milling/1011031.article#ixzz2EUuX9zVB. Last accessed December 2012
7. Gudani R, Shukla M (2012) Controlled depth abrasive water jet cutting of grade 2 titanium and regression modeling. Int J Mech Eng Mater Sci 5(2):117–122
8. Siddiqui TU (2010) Abrasive water jet cutting of continuous fiber-reinforced polymer composites: experimental studies, modeling and multi-objective optimization. Unpublished PhD thesis, MNNIT Allahabad
9. Hashish M (1994) Three-dimensional machining with abrasive waterjets, waterjet cutting technology. Mechanical Engineering Publications, Ltd, London, pp 605–633
10. Kovacevic R, Hashish M, Mohan R, Ramulu M, Kim TJ, Geskin ES (1997) State of the art of research and development in abrasive waterjet machining. Trans ASME 119:776–785
11. Folkes J (2009) Waterjet–an innovative tool for manufacturing. J Mater Process Technol 209(20):6181–6189
12. Fowler G, Shipway PH, Pashby IR (2005) Abrasive water-jet controlled depth milling of Ti6Al4V alloy—an investigation of the role of jet–workpiece traverse speed and abrasive grit size on the characteristics of the milled material. J Mater Process Technol 161:407–414
13. Uhlmann E, Flögel K, Kretzschmar M, Faltin F (2012) Abrasive waterjet turning of high performance materials. In: 5th CIRP conference on high performance cutting 2012, Procedia CIRP 1, pp 409–413
14. Manu R, Ramesh Babu N (2008) Influence of jet impact angle on part geometry in abrasive waterjet turning of aluminium alloys. Int J Mach Mach Mater 3(1/2):120–132
15. Axinte DA, Stepanian JP, Kong MC, McGourlay J (2009) Abrasive waterjet turning—an efficient method to profile and dress grinding wheels. Int J Mach Tools Manuf 49(3–4): 351–356
16. Siddiqui TU, Shukla M (2011) Abrasive waterjet hole trepanning of thick Kevlar-epoxy composites for ballistic applications–experimental investigations and analysis using design of experiments methodology. Int J Mach Mach Mater 10(3):172–186
17. Hashish M (1987) Turning with abrasive waterjets—a first investigation. ASME J Eng Indus 109(4):281–290
18. Hashish M (1991) Characteristics of surfaces machined with abrasive waterjets. J Eng Mater Technol Trans ASME 113(3):354–362
19. Selvan MCP, Raju NMS (2011) Review of the current state of research and development in abrasive waterjet cutting. Int J Adv Eng Sci Technol 11(2):267–275
20. N. Yusup, Zain AM, Hashim SZM (2012) Evolutionary techniques in optimizing machining parameters: review and recent applications (2007–2011). Expert Syst Appl 39:9909–9927
21. Zeng J, Kim TJ (1996) An erosion model of polycrystalline ceramics in abrasive waterjet cutting. Wear 193(2):207–217
22. Paul S, Hoogstrate AM, van Luttervelt CA, Kals HJJ (1998) An experimental investigation of rectangular pocket milling with abrasive water jet. J Mater Process Technol 73:179–188
23. Hashish M, Monserud D (1990) Abrasive waterjet machining of isogrid structures. Quest Integrated Inc., Report QUEST TR-508, pp 63

24. Shipway PH, Fowler G, Pashby IR (2005) Characteristics of the surface of a titanium alloy following milling with abrasive waterjets. Wear 258:123–132
25. Fowler G, Shipway PH, Pashby IR (2008) An investigation of the role of jet impingement angle on process efficiency and surface characteristics for abrasive waterjet milling of Ti6A14V. In: Proceedings of the 19th international conference on water jetting, Nottingham, UK, pp 353–364
26. Hashish M (2008) Waterjet pocket milling of titanium aluminide. In: Proceedings of the 19th international conference on water jetting, Nottingham, UK, pp 365–376
27. Fowler G, Pashby IR, Shipway PH (2009) The effect of particle hardness and shape when abrasive water jet milling titanium alloy Ti6Al4V. Wear 266:613–620
28. Srinivasu DS, Axinte DA, Shipway PH, Folkes J (2009) Influence of kinematic operating parameters on kerf geometry in abrasive waterjet machining of silicon carbide ceramics. Int J Mach Tools Manuf 49:1077–1088
29. Zhu HT, Huang CZ, Wang J, Li QL, Che CL (2009) Experimental study on abrasive waterjet polishing for hard-brittle materials. Int J Mach Tools Manuf 49(7–8):569–578
30. Hloch S, Valicek J (2011) Prediction of distribution relationship of titanium surface topography created by abrasive waterjet. Int J Surf Sci Eng 5(2/3)
31. Dadkhahipour K, Nguyen T, Wang J (2012) Mechanisms of channel formation on glasses by abrasive waterjet milling. Wear 292–293:1–10
32. Pang KL, Nguyen T, Fan JM, Wang J (2012) Modelling of the micro-channelling process on glasses using an abrasive slurry jet. Int J Mach Tools Manuf 53:118–126
33. Rabani A, Marinescu I, Axinte D (2012) Acoustic emission energy transfer rate: a method for monitoring abrasive waterjet milling. Int J Mach Tools Manuf 61:80–89
34. Alberdi A, Rivero A, de Lacalle LNL (2011) Experimental study of the slot overlapping and tool path variation effect in abrasive waterjet milling. J Manuf Sci Eng 133(3):034502
35. Alberdi A, Rivero A, Carrascal A, Lamikiz A (2012) Kerf profile modelling in abrasive waterjet milling. Mater Sci Forum 713:91–96
36. Anwar S, Axinte DA, Becker AA (2013) Finite element modelling of abrasive waterjet milled footprints. J Mater Process Technol 213:180–193
37. Kovacevic R, Yong Z (1996) Modeling of 3D abrasive waterjet machining, part I: theoretical basis, jetting technology. Institution of Mechanical Engineers, pp 73–82
38. Yong Z, Kovacevic R (1996) Modeling of 3D abrasive waterjet machining, part II: simulation of machining, jetting technology. Institution of Mechanical Engineers, pp 83–89
39. Duflou JR, Kruth JP, Bohez EL (2001) Contour cutting of pre-formed parts with abrasive waterjet using 3-axis nozzle control. J Mater Process Technol 115(1):38–43
40. Hashish M (2005) Economics of abrasive-waterjet cutting at 600 MPA pressure. In: Proceedings of WJTA American waterjet conference, Houston, Texas, Paper 4A-3, pp 1–14
41. Hoogstrate AM, Susuzlu T, Karpuschewski B (2006) High performance cutting with abrasive waterjets beyond 400 MPa. CIRP Ann Manuf Technol 55(1):1–4
42. Boud F, Carpenter C, Folkes J, Shipway PH (2010) Abrasive waterjet cutting of a titanium alloy: the influence of abrasive morphology and mechanical properties on workpiece grit embedment and cut quality. J Mater Process Technol 210(15):2197–2205
43. Kong MC, Anwar S, Billingham J, Axinte DA (2012) Mathematical modeling of abrasive waterjet footprints for arbitrarily moving jets: partI—single straight paths. Int J Mach Tools Manuf 53:58–68
44. Palafox GAE, Gault RS, Ridgway K (2012) Characterisation of abrasive water-jet process for pocket milling in Inconel 718. In: 5th CIRP conference on high performance cutting, procedia CIRP 1 (2012), pp 404–408
45. Evans AG, Gulden ME, Rosenblatt ME (1978) Impact damage in brittle materials in the elastic-plastic response regime. Proc R Soc Lon A 361:343–365
46. Abdel-Rahman AA, El-Domiaty AA (1998) Maximum depth of cut for ceramics using abrasive waterjet technique. Wear 218(2):216–222
47. Hassan A, Chen C, Kovacevic R (2004) On-line monitoring of depth of cut in AWJ cutting. Int J Mach Tools Manuf 44:595–605

48. Lemma E, Deam R, Chen L (2005) Maximum depth of cut and mechanics of erosion in AWJ oscillation cutting of ductile materials. J Mater Process Technol 160(2):188–197
49. Wang J (2007) Predictive depth of jet penetration models for abrasive waterjet cutting of alumina ceramics. Int J Mech Sci 49(3):306–316
50. Wang J (2009) A new model for predicting the depth of cut in abrasive waterjet contouring of alumina ceramics. J Mater Process Technol 209(5):2314–2320
51. Kumar N, Shukla M (2012) Finite element analysis of multi-particle impact on erosion in abrasive water jet machining of titanium alloy. J Comput Appl Math 236(18):4600–4610
52. Vikram G, Ramesh Babu N (2002) Modelling and analysis of abrasive waterjet cut surface topography. Int J Mach Tools Manuf 42:1345–1354
53. Hlavac LM (2009) Investigation of the abrasive water jet trajectory curvature inside the kerf. J Mater Process Technol 209(8):4154–4161
54. Kovacevic R, Fang M (1994) Modeling of the influence of the abrasive waterjet cutting parameters on the depth of cut based on fuzzy rules. Int J Mach Tools Manuf 34(1):55–72
55. Srinivasu DS, Ramesh Babu N (2008) A neuro-genetic approach for selection of process parameters in abrasive waterjet cutting considering variation in diameter of focusing nozzle. Appl Soft Comput 8(1):809–819
56. Zain AM, Haron H, Sharif S (2011) Estimation of the minimum machining performance in the abrasive waterjet machining using integrated ANN-SA. Expert Syst Appl 38(7): 8316–8326
57. Zain AM, Haron H, Sharif S (2011) Optimization of process parameters in the abrasive waterjet machining using integrated SA–GA. Appl Soft Comput 11:5350–5359
58. Vundavilli PR, Parappagoudar MB, Kodali SP, Benguluri S (2012) Fuzzy logic-based expert system for prediction of depth of cut in abrasive water jet machining process. Knowledge-Based Systems 27:456–464
59. Kumar N, Shukla M, Patel RK (2010) Finite element modeling of erosive wear in abrasive jet machining. In: International conference on theoretical, applied, computational and experimental mechanics, ICTACEM, IIT Kharagpur, India, Paper 168
60. Hassan AI, Kosmol J (2000) Finite element modeling of abrasive water-jet machining. In: Proceedings of the 15th International conference on jetting technology. Ronneby (Sweden): BHR Group, pp 321–33
61. Junkar M, Jurisevic B, Fajdiga M, Grah M (2006) Finite element analysis of single-particle impact in abrasive water jet machining. Int J Impact Eng 32:7
62. Ahmadi-Brooghani SY, Hassanzadeh H, Kahhal P (2007) Modeling of single-particle impact in abrasive water jet machining. Int J Mech Sys Sci Eng 1:4
63. Takaffoli M, Papini M (2009) Finite element analysis of single impacts of angular particles on ductile targets. Wear 267:144–151
64. Anwar S, Axinte DA, Becker AA (2011) Finite element modelling of a single-particle impact during abrasive waterjet milling. In: Proceedings of the Institution of Mechanical Engineers, part J: Journal of Engineering Tribology, August 2011, vol 225, 8, pp 821–832
65. ElTobgy MS, Ng E, Elbestawi MA (2005) Finite element modeling of erosive wear. Int J Mach Tools Manuf 45:1337–1346
66. Molinari JF, Ortiz M (2002) A study of solid-particle erosion of metallic targets. Impact Eng 27:347–358
67. Shimizu K, Noguchi T, Seitoh H, Okadab M, Matsubara Y (2001) FEM analysis of erosive wear. Wear 250:779–784
68. Liu H http://www.eprints.qut.edu.au/16110/1/Hua_Liu_Thesis.pdf
69. Wang R, Wang M (2010) A two-fluid model of abrasive waterjet. J Mater Process Technol 210(1):190–196
70. Arcam Titanium Grade 2 (2012) www.arcam.com/CommonResources/Files/arcam.com/Documents/EBM%20Materials/Arcam-Titanium-Grade-2.pdf. Last accessed December 2012
71. Flow Mach 4 AWJ machines (2012) http://www.flowwaterjet.com/en/waterjet-cutting/cutting-systems/mach-4.aspx. Last accessed December 2012
72. www.precisionmachinerysales.com/waterjet/1392.htm. Last accessed December 2012

73. http://www.sawaterjet.co.za/photo_gallery/index2.html. Last accessed December 2012
74. Momber AW, Kovacevic R (1998) Principles of abrasive water jet machining. Springer, London
75. Montgomery DC (2001) Design and analysis of experiments, 5th edn. Oxford Publications, New York
76. Wang J (2007) Predictive depth of jet penetration models for abrasive waterjet cutting of alumina ceramics. Int J Mech Sci 49:306–316
77. Siddiqui TU, Shukla M (2010) Modeling of depth of cut in abrasive waterjet cutting of thick kevlar-epoxy composites. Key Eng Mater 443:423–427
78. NLREG (2012) www.nlreg.com. Last accessed December 2012
79. Minitab (2012) www.minitab.com. Last accessed December 2012
80. Alberdi A, Rivero A, López de Lacalle LN, Suárez A (2010) Effect of process parameter on the kerf geometry in abrasive water jet milling. Int J Adv Manuf Technol 51:467–480
81. Shukla M, Tambe PB (2013) Genetic algorithm based optimization of material removal rate with surface finish constraints in abrasive water jet cutting of carbon-epoxy composites. Accepted in Natural Computing
82. Siddiqui TU, Shukla M (2012) Modeling and optimization of abrasive water jet cutting of kevlar fiber-reinforced polymer composites, in "computational methods for optimizing manufacturing technology—models and techniques". IGI Global, USA, pp 262–286
83. Shukla M, Tambe PB (2010) Predictive modeling of surface roughness and kerf widths in abrasive water jet cutting of kevlar composites using neural network. Int J Mach Mach Mater 8(1 & 2):226–246
84. Borkowski J (2010) Application of abrasive-water jet technology for material sculpturing. Trans Can Soc Mech Eng 34(3–4):389–398